Characterizing the Inhomogeneity of Aorta Mechanical Properties and its Effect on the Prediction of Injury

Golriz Kermani, Soroush Assari, Ali Hemmasizadeh, Kurosh Darvish
Biomechanics Lab, Department of Mechanical Engineering, Temple University

ABSTRACT

Traumatic aortic rupture (TAR) is one of the most significant causes of motor-vehicle fatalities with the majority of injuries occurring in the peri-isthmus region. Despite the fact that TAR accounts for 20% of the total automobile fatalities, there is uncertainty regarding its etiology and underlying mechanisms. Finite element (FE) models are essential for calculating the strains and stresses in aorta during car accidents leading to TAR and assessing the risk of injury and/or failure. Current FE models of the thorax generally consist of simplistic material models for the aorta with the assumptions of isotropy and homogeneity. In order to develop reliable FE models, suitable constitutive relationships are needed which account for the rate dependency, nonlinearity, inhomogeneity, and anisotropy of the aortic tissue. The objectives of this study were twofold. The first objective was to investigate the inhomogeneity of porcine descending thoracic aorta (DTA) using a custom-made nano-indentation test setup. The second objective was to investigate the risk of aortic failure in car accidents by implementing the inhomogeneity of aorta in the Global Human Body Model (GHBM). Changes in stress and strain distributions and the effect of aortic inhomogeneity were evaluated in frontal chest impacts. The results from nano-indentations in the axial orientation showed that distal sections are stiffer than the proximal ones and the medial quadrant shows the least stiff behavior. Results from FE simulations suggest that implementing the inhomogeneity of the aortic tissue had the most influence on the isthmus and ATA regions.

INTRODUCTION

Traumatic Aortic Rupture (TAR) is the 2nd most common cause of fatal injuries observed in automotive accidents only after traumatic brain injury with survival rates of less than 10% in the field and less than 2% overall (Plummer et al. 2006; Richens et al. 2003). Consequently mitigation and prevention of TAR is of paramount importance. Despite the fact that TAR is a significant public health problem, there is still uncertainty regarding the etiology and mechanisms of this injury. Various hypotheses have been proposed for the mechanisms of TAR including longitudinal stretching, intravascular pressure, osseous pinch, and water hammer effect (Richens et al. 2002). However, since experimental reproductions of such complex loadings and deformations in cadaveric surrogate tests have been inconclusive (Cavanaugh et al. 2005), finite element (FE) modeling is the preferred method to gain a better insight into the mechanisms of TAR as a result of human blunt chest trauma.

With advancements in medical imaging techniques, the geometry of current FE models of human body for trauma applications (e.g., the GHBMC model) is highly accurate. However, in terms of materials properties, these models are still simplistic. For example, in the GHBMC model the aorta is assumed to be homogeneous, isotropic, and linearly elastic while experimental results at the tissue level show that it is inhomogeneous, anisotropic, nonlinear, and viscoelastic (Mohan & Melvin 1983; Shah et al. 2006; Sokolis et al. 2008). Therefore, characterizing the anisotropy and inhomogeneity of aortic tissue is necessary to improve the TAR FE models and in better elucidating the mechanisms of TAR, improving car safety and injury prevention considerations, and clinical treatment of the injury.

Few studies have focused on the inhomogeneous behavior of aorta in the longitudinal and circumferential directions. Sokolis et al., (2008) studied the regional aortic elastic properties under low, physiological, and high states of stress by conducting uniaxial tensile tests on longitudinal strips of porcine aorta, excised from 4 locations along the thoracic aorta. Their results showed that the biomechanical characteristics and composition of aortic wall were nonhomogeneous and the proximal sections of the aortic wall showed more compliant behavior than the distal ones at physiologic and high stresses. The only study investigating the inhomogeneity of the aorta in the circumferential direction was conducted by Choudhury et al., (2009) on healthy and dilated human ascending aorta using equi-biaxial tests. Their results showed that the stiffest and the least stiff parts of the aortic wall were on the lateral and medial quadrants, respectively.

FE Analysis has been used previously to investigate the mechanisms of TAR in simulated automotive crashes (Shah et al. 2001; Richens et al. 2004; Belwadi et al. 2012). One of the first detailed FE models of human chest was developed by Shah et al. (2001) in order to simulate seven impact tests at the level of T8 at 30-degree intervals. The peri-isthmus region experienced the highest principal stresses in all impact scenarios. In frontal impacts, the isthmus, the ATA and mid-DTA were most likely to rupture. Richens et al., (2004) developed a thorax model and extracted the motion response of the heart following a simulated thoracic frontal impact and applied it in a second more detailed FE model of the heart and aorta in order to investigate the stresses experienced by the aortic isthmus. Maximum stresses occur at the isthmus and pulmonary artery bifurcation. Belwadi et al., (2012) reconstructed eight near side lateral impacts, where TAR occurred, using the Crash Injury Research and Engineering Network (CIREN) database, FE models of vehicles, and the Wayne State Human Body Model–II (WSHBM). Their results showed that the peak maximum principal strains occurred in the peri-isthmus region. In the above mentioned studies aortic behavior is considered to be linear, isotropic, and rate independent.

The objectives of this study were twofold. First objective was to characterize the inhomogeneity of the aortic tissue at various quadrants on the circumferential aortic ring and at various sections along the aortic tree. In order to address this, nano-indentation tests were conducted on porcine descending thoracic aorta (DTA) in axial orientation. The second objective was to investigate the effect of the inhomogeneity of TA on the assessment of injury. For this purpose, the Global Human Body Models Consortium (GHBMC) mid-sized male model was used and the stress and strain distributions were evaluated and compared due to frontal chest impacts. The results of this study can be used to explain the mechanisms of deformation and will contribute to improving computational modeling and prediction of aortic failure.

METHODS

Nano-indentation tests

Fresh porcine DTA specimens were excised from seven pigs. Six transverse rings, 8-10 mm in length, were excised after cleaning the specimens from fat and excessive tissues. The specimens were divided into sections according to their location along the aortic tree. Upper-DTA, mid-DTA, and lower-DTA were above the 1st intercostal artery, between the 1st and the 2nd intercostal arteries, and between the 3rd and 4th intercostal arteries, respectively. To investigate the effect of circumferential location (θ-direction), anterior, posterior, medial, and lateral quadrants were marked on the specimens. Indentations in the axial orientation were conducted along the aorta thickness moving from the inner wall to the outer wall for each of the mentioned samples using a custom-designed nano-indentation setup. Samples were moved upward toward the indenter with a ramp and hold displacement with 60 μm indentation depth, 25 ms ramp time and 20 s hold time using a LabVIEW-driven motion control system.

Formulation. The viscoelastic behavior were characterized using a Quasi-Linear Viscoelastic (QLV) model. For a conical indenter with the semi-vertical angle of β (= 62.5°), the relationship between the indenter force history, $P(t)$, and the indentation depth, $h(t)$, is given by (Sneddon 1965; Hemmasizadeh et al. 2012):

$$P(t) = \int_0^t G(t-\tau)(\partial P^e(h)/\partial h)(\partial h)/\partial \tau) d\tau \qquad (1)$$

$$G(t) = G_\infty + \sum_{i=1}^{4} G_i \exp(-\beta_i t) \qquad (2)$$

$$P^e = (1/\alpha)\{2E cot(\beta)/\pi(1-\nu^2)\} h^2 \qquad (3)$$

in which $P^e\ (h)$ is the instantaneous elastic force and $G(t)$ is the reduced relaxation function. G_i and $\beta_{1..4} = 0.1, 1, 10, 100\ s^{-1}$ are the reduced relaxation amplitudes and decay rates, respectively. E is the instantaneous Young's modulus, and ν is the Poisson's ratio which was assumed to be 0.49 (almost incompressible) for fresh aorta. The nano-indentation test results were calibrated using the previous study where a correction factor, α, was determined based on the comparison between conical and flat indenter results (Hemmasizadeh et al. 2012). The correction factor depended on the indentation depth and was approximately equal to 3 for the indentation depth used in this study (h = 60 μm).

Statistical analysis. Statistical analysis was performed, using JMP SAS, Version 11, Cary, NC, to test for significant dependence of the viscoelastic parameters on z- and θ-directions. Multi-variate analysis of variance (MANOVA) followed by the Tukey's HD test were used and significance threshold of 0.05 was considered for the p-value.

FE model

Commercially available FE model, GHBMC Full Body Model of the 50th percentile male (M50, V4.1) was used in this study to investigate the effect of biomechanical properties of aortic tissue on the risk of aortic injury. All simulations were run using LS-DYNA (R. 4.2.0; LSTC, Livermore, CA) at Temple University. In the original model, the aorta is modeled with shell elements, filled with solid fluid, and as linear elastic material. Current GHBM is limited by considering non-realistic mechanical properties and simplifying assumptions of homogeneity, isotropy, and linear elasticity of the aorta. Table 1 lists the material characteristics of aorta, heart, and blood in the original model.

Table 1: Material characteristics of the thorax model in original GHBM

Tissue	Material Model (ID)	Material Coefficient
Aorta	Elastic (1)*	$\rho = 1.2\ g/cm^3,\ E = 8.87\ MPa,\ v = 0.4$
Heart	Hyperelastic (128) **	$C = 1.085\ kPa, B_1 = 24.26, B_2 = 40.52, B_3 = 1.63, P = 2.4825\ GPa$
Blood	Elastic fluid (1)	$\rho = 1.0\ g/cm^3, \quad K = 2.2\ MPa, \quad v = 0.45$
* Yuen, (2009)	** Deng et al., (1999)	

Current GHBM assumes a homogeneous model (HM) for the aorta with E = 8.87 MPa. In order to make an inhomogeneous model along the aortic tree (IHM_L), TA was divided into 5 sections according to their location: ATA, aortic arch, upper-DTA, mid-DTA, and lower-DTA (Figure 1-a). The circumference of the TA at each section, was further divided into 4 regions, i.e., anterior, lateral, medial, and posterior quadrants, to implement the inhomogeneous model in the θ-direction (IHM_{LC}), (Figure 1-b). In order to compare the response of various sections, the section of the aortic arch just distal to the origin of the left subclavian artery is referred to as the Isthmus, and the section of the aortic arch next to the ATA is referred to as the Arch.

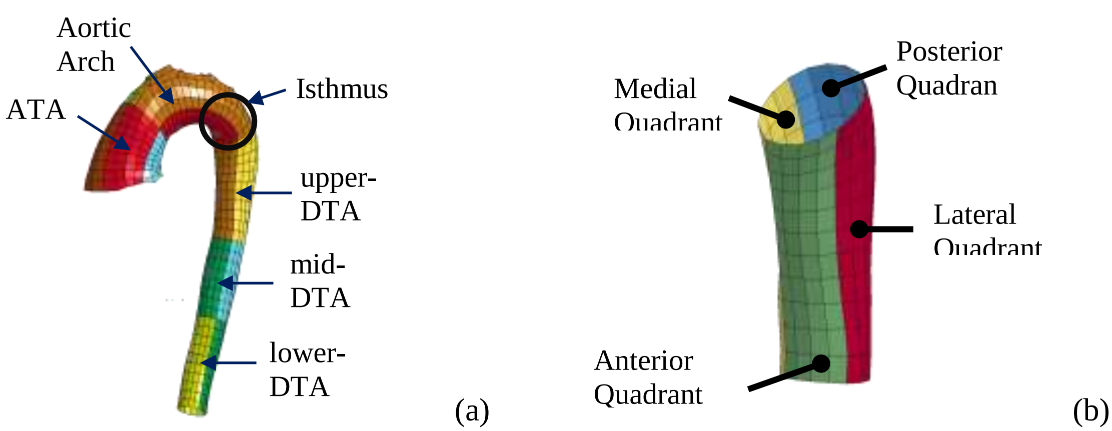

Figure 1: Schematic representation of a) IHM_L and b) IHM_{LC}.

The lower-DTA generally shows the stiffest response, therefore the average value for this section was chosen to be the same as HM and as a base for implementing the inhomogeneity. The ratios were calculated based on nano-indentation tests and other studies found in the literature (Sokolis et al. 2008; Choudhury et al. 2009). It should be noted that the results from nano-indentation tests represent the aortic behavior at low-stress ranges. The linear elastic material model (LS-DYNA's MAT_001) was considered for each section based on the existing material properties. The GHBM assumes a stiff response for the aorta for instability issues.

Frontal Kroell-type chest impact tests were simulated at 4.3 m/s in the driver position and the time histories of effective (von-Mises) stress and strain, indicating the aortic dynamic response, were plotted at various sections and quadrants of the TA. The results were compared with the HM with E = 8.87 MPa and the regions experiencing high stresses and high strains were identified and considered to be more prone to rupture. Four adjacent elements in the region of interest were selected and the corresponding stresses and strains were averaged and used for comparison.

RESULTS

The QLV material properties were determined by optimizing for G_i and E to fit the experimental data. There was generally an increase in the elastic moduli from proximal to distal aortic sections (Figure 2-a). Lower-DTA was statistically stiffer than upper- and mid-DTA (p = 0.01 and <0.0001, respectively). The medial quadrant showed the most compliant behavior compared to other quadrants (p < 0.0001) as shown in Figure 2-b. The ratios of the stiffness values between different sections and quadrants were calculated based on nano-indentation results for the lower-DTA section and applied to 8.87 MPa to obtain the material properties of the inhomogeneous models (Table 2 and 3).

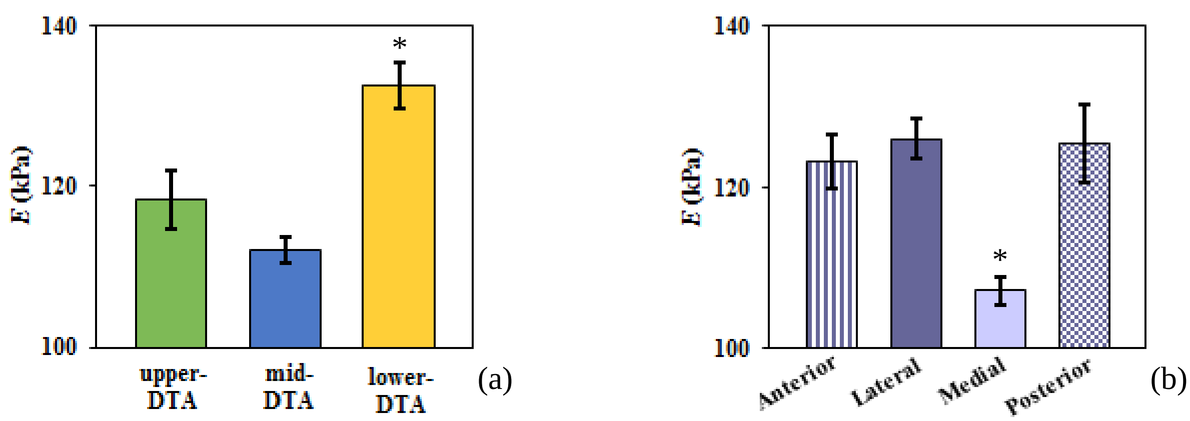

Figure 2: Variation of E in the a) z-direction and b) θ-direction. Error bars represent the standard error of the mean.

Table 2: Aorta elastic modulus in IHM_L (MPa)

Section	ATA	Arch	upper-DTA	mid-DTA	lower-DTA
***E* (MPa)**	5.79 [1]	6.03 [2]	7.85 [2]	7.56 [2]	8.87 [3]

[1]Choudhury et al., (2009) [2] This Study [3] GHBM

Table 3: Aorta elastic modulus in IHM_{LC} (MPa)

Section	Anterior	Lateral	Medial	Posterior
ATA	5.26	7.28	3.49	7.14
Aortic Arch	6.26	7.63	7.92	7.26
upper-DTA	6.26	7.63	7.92	7.26
mid-DTA	7.27	8.02	6.75	7.38
lower-DTA	9.93	9.04	7.05	10.24

Representative distributions of effective stress and strain for HM, IHM_L, and IHM_{LC} are shown in Figure 3 at the isthmus section, medial quadrant. It can be seen that implementing the inhomogeneity of the aorta changed the absolute value of the stresses and strains, but the pattern of their distribution did not change. The peak stress value in the isthmus region was decreased by 22% in the IHM_L compared with the HM. In the case of effective strain, the peak increased by 18%.

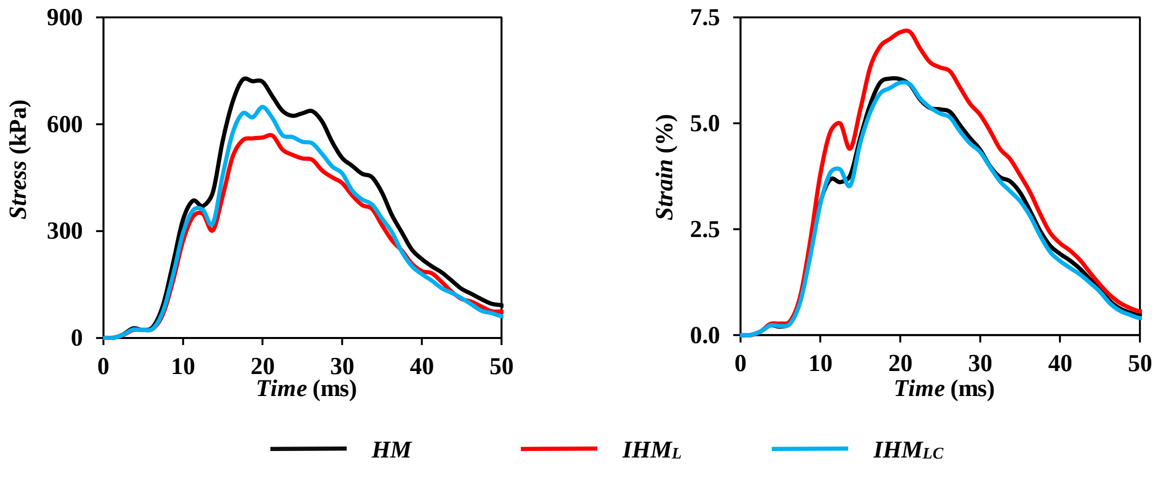

Figure 3: Effective stress and strain response of the isthmus section due to a frontal chest impact at 4.3 m/s.

The peak values of the maximum effective stress and strain in various sections along the aortic tree are listed in Tables 4 and 5. In all cases except the IHM_{LC}, the Arch section experienced the highest stress, followed by the Isthmus section. In the IHM_{LC}, the regions of high stress were observed at the Isthmus and Arch (648.4 and 624.5 kPa, respectively). The comparison of the effective strain results showed that the highest strain occurred at Isthmus section in HM and IHM_L (6.1% and 7.1%, respectively), while ATA section experienced the highest peak strain value in IHM_{LC} (7.4%). These results suggest that the isthmus and ATA sections are more sensitive to changes in aortic properties and implementing the inhomogeneous model. Implementing patient-specific aortic material properties would be a crucial step in improving the FE models and elucidating the deformation mechanisms due to crashes.

Table 4: Average peak values of effective stress in kPa predicted by the HM, IHM_L, and IHM_{LC} at different sections

	lower-DTA	mid-DTA	upper-DTA	Isthmus	Arch	ATA
HM	509.8	552.0	340.1	724.3	791.3	509.4
IHM_L	509.2	537.2	327.7	567.9	590.3	382.2
IHM_{LC}	462.9	505.2	326.1	648.4	624.5	385.0

Table 5: Average peak values of effective strain in % predicted by the HM, IHM_L, and IHM_{LC} at different sections

	lower-DTA	mid-DTA	upper-DTA	Isthmus	Arch	ATA
HM	4.6	4.1	2.8	6.1	3.6	5.6
IHM_L	4.4	4.4	3.0	7.1	4.3	6.5
IHM_{LC}	4.6	4.6	3.5	6.0	4.2	7.4

DISCUSSION

Comparison between experimental data and QLV model prediction showed that this model was capable of characterizing the behavior of the aortic tissue. The statistical analysis showed that E were dependent on z- and θ- directions. The distal sections showed a significantly stiffer response compared with the proximal ones which is in agreement with previous studies (Sokolis, 2008) where this variation was correlated with the decrease in the elastin content, and increase in the collagen content. The medial quadrant exhibited the most compliant behavior. A previous study of the variation of mechanical properties of human ATA with θ showed that the medial and the lateral quadrants were the least stiff and the stiffest locations, respectively (Choudhury, 2009). Nano-indentation tests showed that the proximal sections and the medial quadrant of aorta were more compliant and consequently sustain higher strains in identical loading scenarios. Based on previous studies (Mohan & Melvin 1983) aortic failure is strain based. Therefore, our results suggest that the medial quadrant, closer to the aortic arch, can be more prone to rupture in an axial loading.

We have implemented the inhomogeneity of the aorta in the GHBM model, and examined its influence on aortic response in frontal chest impacts. States of effective stress and strain were calculated at six sections along the aortic tree and the results suggest that the Isthmus region is affected the most by the inhomogeneous model. This would mean that when person to person variability in aorta material properties is taken into account, it is expected that the stresses and strain in the isthmus would be mostly affected and confirms why this region is more prone to failure.

Limitations – future work. One of the limitations of this study is the use of porcine aorta in nano-indentation experiments, which is representative of healthy and young human aorta. Therefore the results should be used with care when dealing with samples affected by age and diseases such as atherosclerosis.

It is necessary to develop more biofidelic FE models in order to investigate various scenarios of trauma by implementing more accurate material models. Further work is needed to add the anisotropy and the radial inhomogeneity of the aorta in the model. In order to apply the results of the nano-indentation experiments in the FE model, it was assumed that the degree of inhomogeneity of DTA did not change with strain. The nonlinearity of the aortic response should be considered. In current GHBMC model, the material properties of other major vessels such as left pulmonary artery, superior vena cava, carotid and subclavian arteries are the same as the aorta. More exact models and properties should be assigned to these components. Additionally, blood is modeled as an elastic fluid which cannot sustain large deformations. Techniques such as Arbitrary Lagrangian Eulerian (ALE) or Smooth Particle Hydrodynamics (SPH) methods can be used to model the blood response as well as its interaction with the aorta.

CONCLUSIONS

Using a custom-made nano-indentation setup, changes in the mechanical properties of porcine DTA from axial indentations were characterized at various locations along the aorta and on the aortic ring with a quasi-linear viscoelastic model. The proximal sections and the medial regions of aorta are more compliant and therefore experience higher strains under identical loading conditions. The results from the FE model suggest that it is important to develop more accurate material models and implement the inhomogeneous biomechanical behavior of the aorta in computational models, in order to gain better insight into the mechanisms of deformation and failure.

ACKNOWLEDGEMENTS

This work was partially supported by AHA under Grant Number 15PRE25090213 (SA) and NHLBI under Grant numbers K25 HL086512-05 and R21 HL088159-02 (KD).

REFERENCES

Belwadi, A. et al., 2012. Finite element aortic injury reconstruction of near side lateral impacts using real world crash data. *Journal of biomechanical engineering*, 134(1), p.011006.

Cavanaugh, J.M. et al., 2005. An Analysis of Traumatic Rupture of the Aorta in Side Impact Sled Tests. , 2005(724).

Choudhury, N. et al., 2009. Local mechanical and structural properties of healthy and diseased

human ascending aorta tissue. *Cardiovascular Pathology*, 18(2), pp.83–91.
Deng, Y.C., Kong, W. & Ho, H., 1999. Development of a finite element human thorax model for impact injury studies. *SAE International Congress and Exposition*.
Hemmasizadeh, A., Autieri, M. & Darvish, K., 2012. Multilayer material properties of aorta determined from nanoindentation tests. *Journal of the Mechanical Behavior of Biomedical Materials*, 15, pp.199–207.
Mohan, D. & Melvin, J.W., 1983. Failure Properties of Passive Human Aortic Tissue. II-Biaxial Tension Tests. *J. Biomechanics*, 16, pp.31–44.
Plummer, D. et al., 2006. Endovascular repair of traumatic thoracic aortic disruption. *Perspectives in vascular surgery and endovascular therapy*, 18(2), pp.132–9.
Richens, D. et al., 2004. A finite element model of blunt traumatic aortic rupture. *European journal of cardio-thoracic surgery : official journal of the European Association for Cardio-thoracic Surgery*, 25(6), pp.1039–47.
Richens, D. et al., 2003. Rupture of the aorta following road traffic accidents in the United Kingdom 1992–1999. The results of the co-operative crash injury study. *European Journal of Cardio-thoracic Surgery*, 23, pp.143–148.
Richens, D. et al., 2002. The mechanism of injury in blunt traumatic rupture of the aorta. *European Journal of Cardio-thoracic Surgery*, 21(2), pp.288–293.
Shah, C.S. et al., 2001. Development of a computer model to predict aortic rupture due to impact loading. *Stapp car crash journal*, 45, pp.161–82.
Shah, C.S. et al., 2006. Dynamic biaxial tissue properties of the human cadaver aorta. *Stapp car crash journal*.
Sneddon, I.N., 1965. The relation between load and penetration in the axisymmetric boussinesq problem for a punch of arbitrary profile. *International Journal of Engineering Science*, 3(1), pp.47–57.
Sokolis, D.P., Boudoulas, H. & Kerayannacos, P.E., 2008. Segmental differences of aortic function and composition: clinical implications. *Hellenic journal of cardiology : HJC = Hellenike kardiologike epitheorese*, 49(3), pp.145–154.
Yuen, K.F., 2009. *The Development of a Numerical Human Body Model for the Analysis of Automotive Side Impact Lung Trauma*.